Elucidating time-resolved intracellular metabolic dynamics via label-free Raman microspectroscopy and 2D correlation spectroscopy

Zohreh Mirveis [1,2], Nitin Patil [1,2], Hugh J. Byrne[1]*

[1]FOCAS Research Institute, TU Dublin, City Campus, Camden Row, Dublin 8, Ireland
[2]School of Physics, Optometric and Clinical Sciences, TU Dublin, City Campus, Grangegorman, Dublin 7, Ireland
*D21127294@mytudublin.ie

1- Preprocessing of Raman spectral data

Raw spectra of cells fed with glucose only at the zero time point are shown in Figure S1-a, with the same procedure applied to all datasets. A Savitzky–Golay filter (polynomial order 5, frame length 9) was first applied to reduce high-frequency noise (Figure S1-a,b). Spectra were then corrected using the adapted Extended Multivariate Signal Correction (EMSC) algorithm[1], which separates true signal from background contributions such as glass. Reference spectra of glass (Figure S1-c) and albumin (Figure S1-d) were incorporated to model the raw spectra as a weighted sum of baseline and reference components. The fitted background (Figure S1-e), consisting of a polynomial baseline plus weighted contributions from glass and albumin, was subtracted to yield background-corrected spectra for further analysis (Figure S-f).

The most appropriate polynomial order for EMSC was established by evaluating its effect on PCA clustering and loadings (Figure S2). Lower orders (N = 2–3) produced dispersed PCA score distributions, reflecting incomplete baseline removal (Figure S2-a). With increasing order, clusters progressively converged, with minimal improvement beyond N = 5. Analysis of PC1 loadings (Figure S2-b) supported this: at low orders, broad baseline features dominated, while sharper biochemical peaks (e.g., ~1350 and ~1750 cm^{-1}) emerged from N = 4 onward and stabilised at N = 5. Thus, polynomial order 5 was selected as the optimal balance between effective baseline correction and preservation of meaningful spectral features.

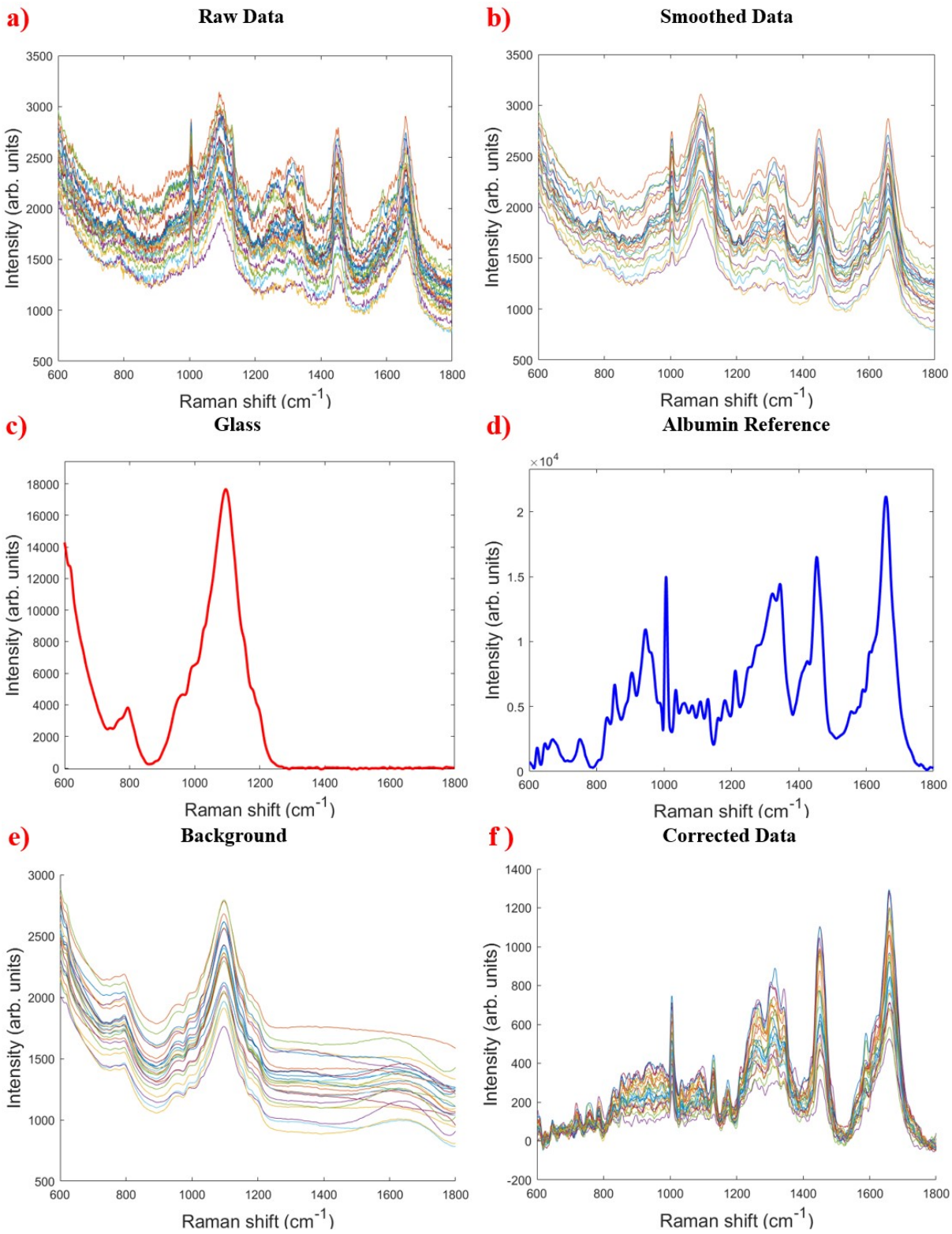

Figure S1. Preprocessing workflow for Raman spectra data. (a) Raw spectra of cells fed with glucose only at the zero time point. (b) Smoothed spectra after applying a Savitzky–Golay filter (polynomial order 5, frame length 9). (c) Glass spectrum used as substrate reference. (d) Albumin spectrum used as biochemical reference. (e) Fitted background consisting of polynomial baseline, glass, and albumin contributions. (f) Background-corrected spectra after EMSC preprocessing.

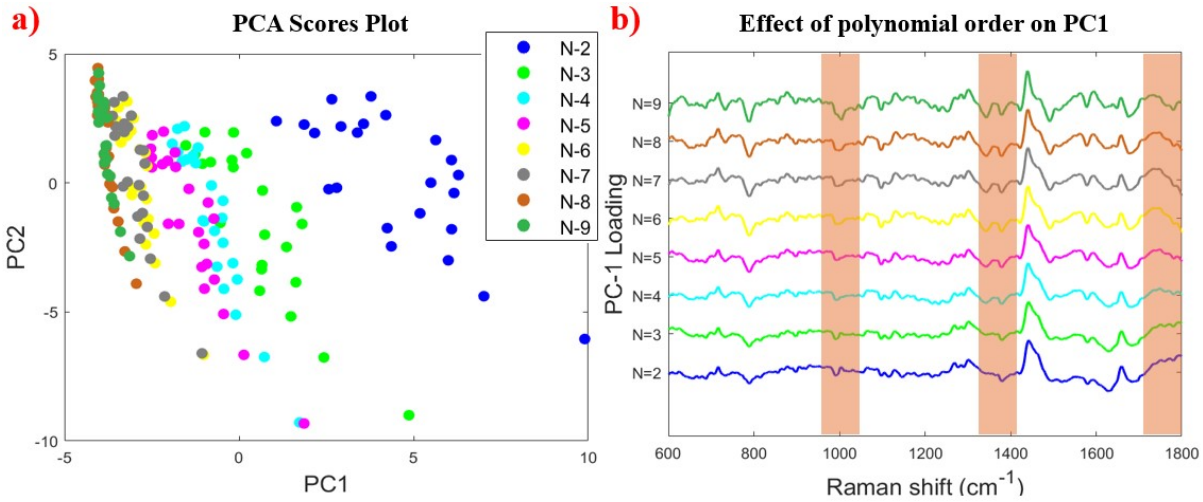

Figure S2. Optimisation of polynomial order for EMSC correction. (a) PCA scores of blank spectra at the zero time point across polynomial orders N = 2–9. (b) PC1 loadings across polynomial orders (N = 2–9).

2. 2D-Correlation spectroscopy analysis

Simulated data representative of the glycolysis pathway were analysed using the 2D correlation spectroscopy (2D-COS) technique. From the synchronous auto-correlation, all variable peaks identified on the diagonal map and their temporal evolution profiles are shown in Figure S3. Panel (a) displays the raw trajectories of all replicates at each time point, while panel (b) presents the averaged profiles for clearer visualisation. These results confirm that several peaks exhibit similar trends, consistent with their assignment to the same components.

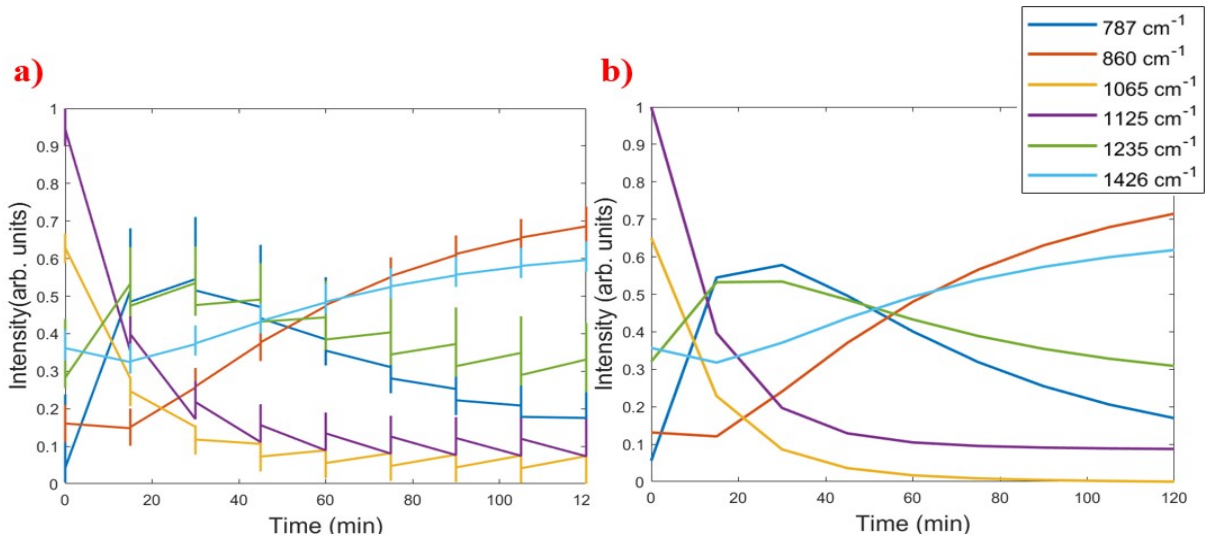

Figure S3. Temporal evolution of the most variable peaks identified from the synchronous map (diagonal peaks), shown with all replicates at each time point (a) and as averaged profiles across time points for clearer visualization (b).

2.1. Testing 2D-COS sensitivity with increasing cellular background (10, 20, 40)

a) **Cellular weight = 10**

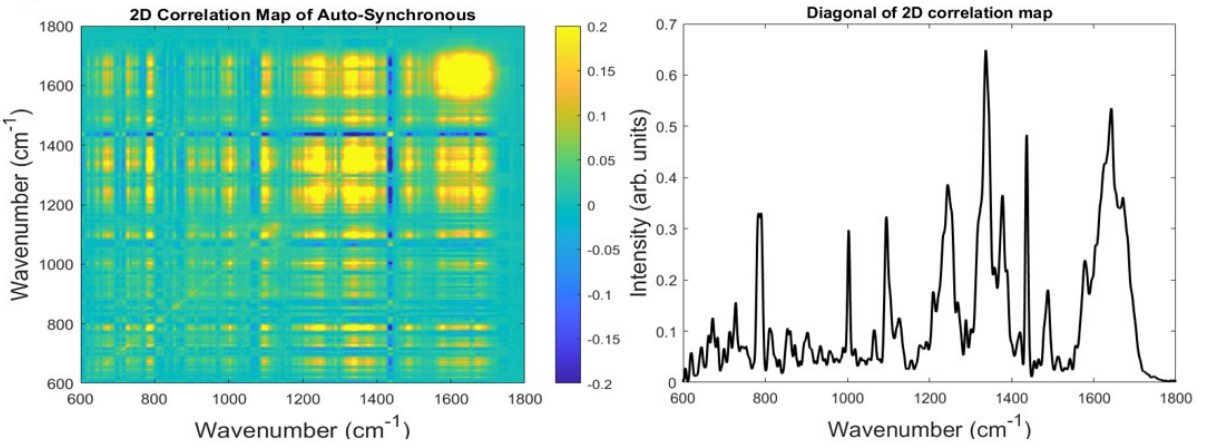

b) **Cellular weight = 20**

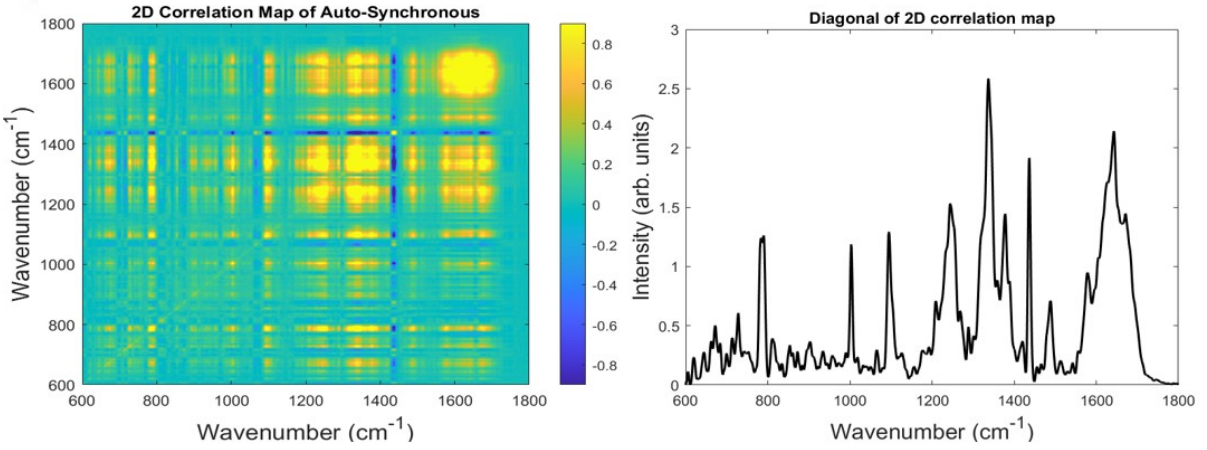

c) **Cellular weight = 40**

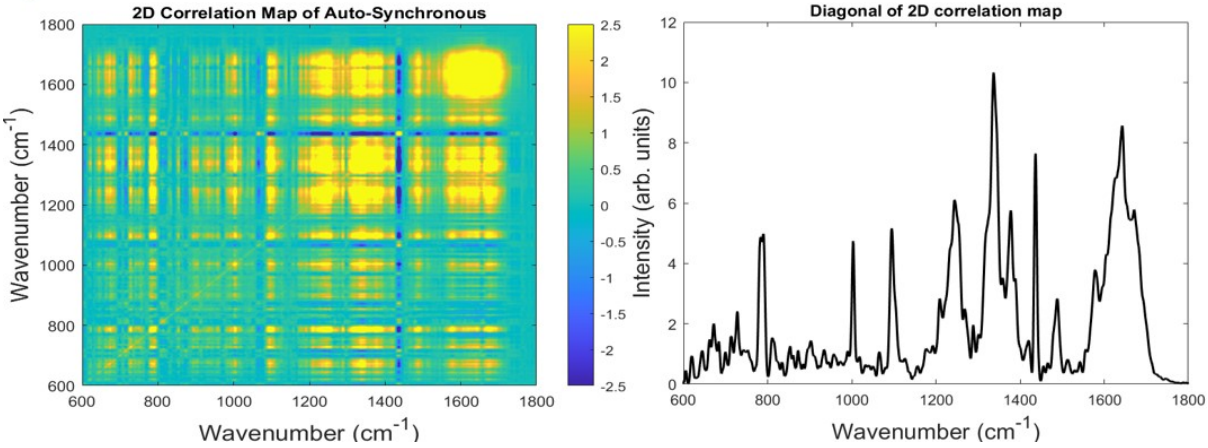

Figure S4. Auto-synchronous maps of simulated glycolysis pathway analysis (left) and their corresponding diagonal plots (right) at different cellular background weights: (a) weight = 10, (b) weight = 20, and (c) weight = 40.

2.2. Distinguishing background signals from dynamic variables

At high levels of cellular background contribution, where the main variations become more subtle, 2D-COS also captures peaks arising from the background (e.g., 1000, 1337, and 1650 cm^{-1}). However, their temporal evolution remains relatively flat compared with the main variable peaks, indicating only a minimal contribution to the dynamic response.

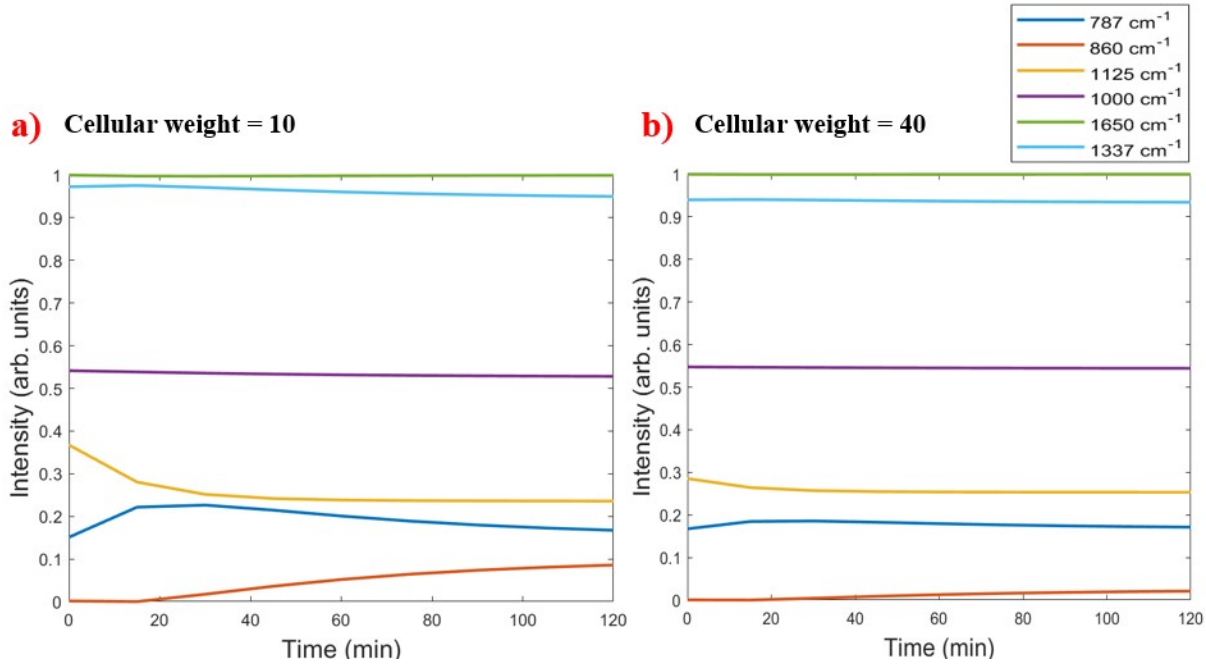

Figure S5. Temporal evolution of selected peaks under increasing cellular background. (a) Cellular weight = 10 and (b) Cellular weight = 40. The peaks at 1000, 1337, and 1650 cm^{-1}, associated with cellular background, show relatively flat temporal evolution compared with the main variables.

2.3. 2D-COS analysis of the simulated model representing glycolysis–glutaminolysis interplay

The 2D-COS results of the simulated glycolysis–glutaminolysis interplay model (A → C, B → C) are shown in Figure S6. Although glucose and glutamine both decrease over time with overlapping signals, the key variable peaks at 855 cm^{-1} (lactate), 1132 cm^{-1} (glucose), and 1333 cm^{-1} (glutamine) are well resolved in the auto-synchronous map, and their temporal evolution can be reliably tracked.

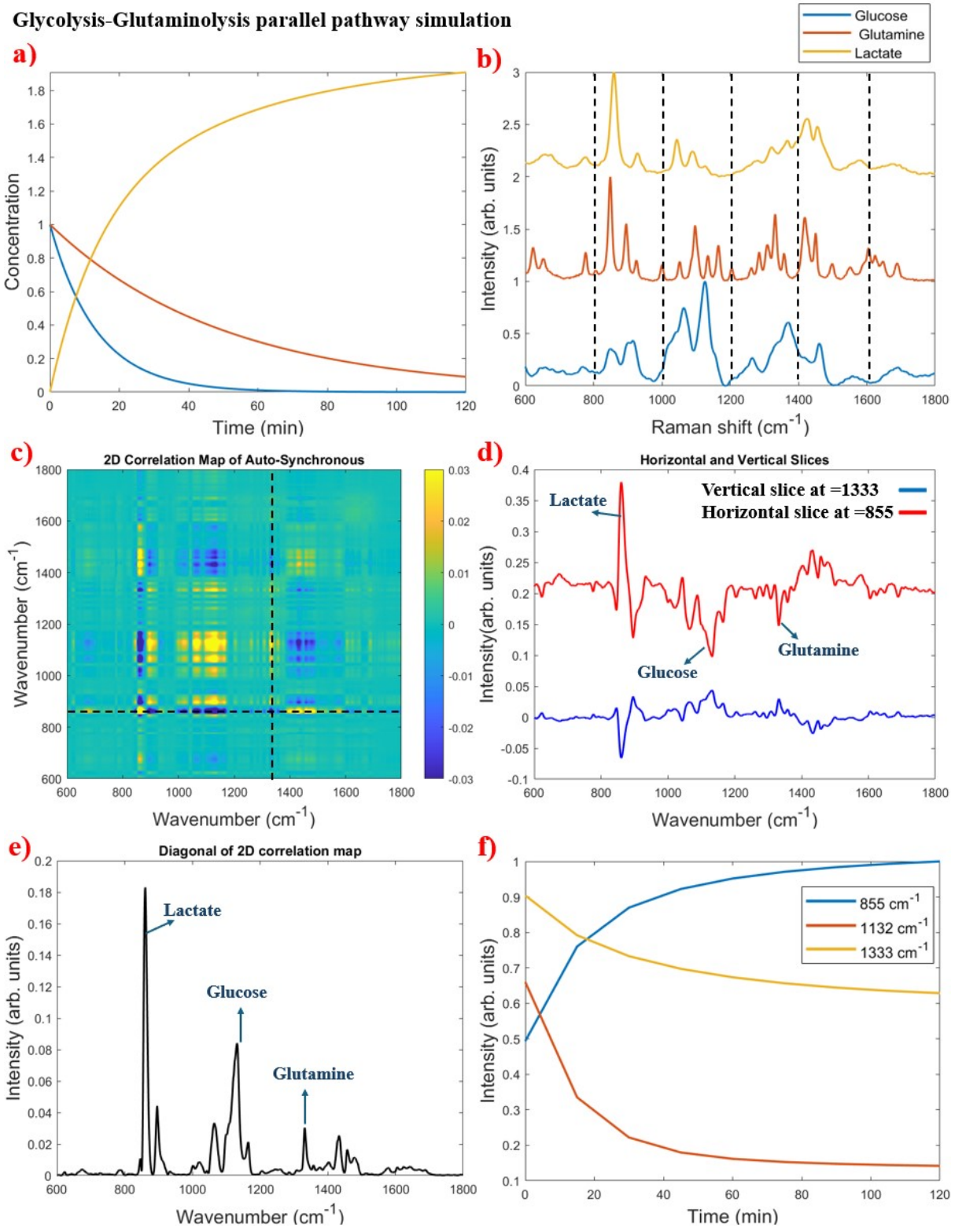

Figure S6. Simulated glycolysis–glutaminolysis interplay model analysed by 2D correlation spectroscopy. (a) Simulated concentration profiles of glucose, glutamine, and lactate. (b) Corresponding spectral signatures. (c) Auto-synchronous 2D-COS map. (d) Representative vertical and horizontal slices at 1333 and 855 cm^{-1}. (e) Diagonal plot identifying the strongest variable peaks. (f) Temporal evolution of representative bands at 855 cm^{-1} (lactate), 1132 cm^{-1} (glucose), and 1333 cm^{-1} (glutamine).

3. 2D-COS analysis of Raman spectral profiles of intracellular metabolism under two different nutritional conditions

Raman spectral data obtained from monkey kidney cells (LLC-MK2) exposed to two different nutritional conditions, glucose alone and a glucose–glutamine mixture, were analysed using 2D-COS. All peaks identified from the auto-synchronous diagonal plots were tracked over time to compare the kinetic evolution under the two conditions. The corresponding plots, showing all replicates at each time point together with averaged trends for clearer visualisation, are presented in Figure S7.

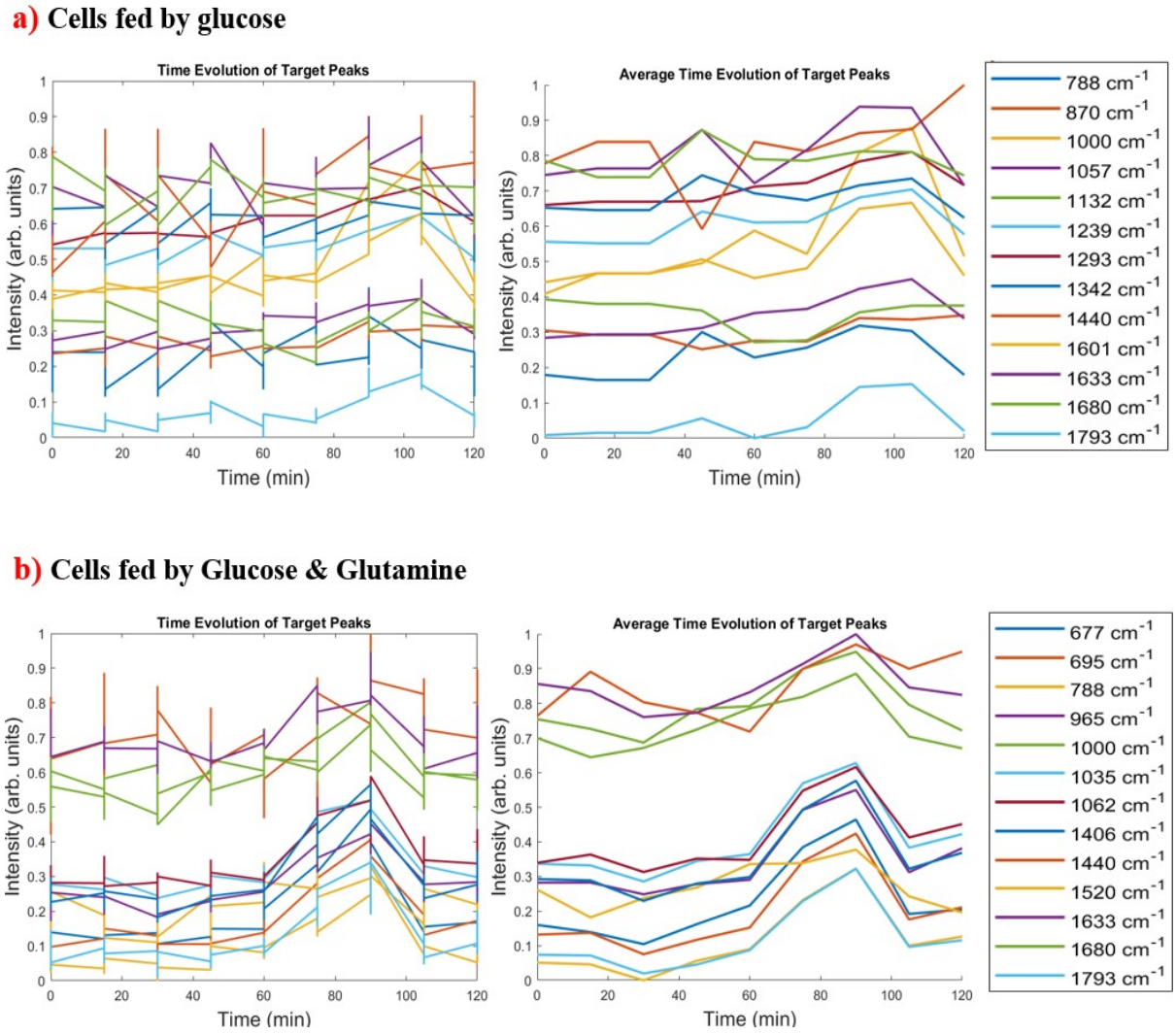

Figure S7. Diagonal peaks identified from the auto-synchronous maps of Raman spectra for cells fed with (a) glucose alone and (b) a glucose–glutamine mixture. The left panels show the time evolution of peaks including all replicates, while the right panels display averaged profiles across time points for clearer visualisation.

Table S1. Assignments of variable peaks identified by 2D-COS in Raman spectra of LLC-MK2 cells exposed to different nutritional conditions (glucose vs. glucose–glutamine)[2–4]

Nutritional Condition	Band (cm^{-1})	Biochemical group	Vibrational assignment
Glucose	788	Nucleic acids	O–P–O stretching, DNA/RNA backbone, ring breathing
	1239	Proteins	Amide III (C–N stretching, N–H bending)
	1342	Proteins	CH_2 wagging, Amide III (proteins)
	1601	Proteins	Aromatic ring vibrations (Tyr, Phe)
	1633	Proteins	Amide I (β-sheet C=O stretching)
	1680	Proteins	Amide I (β-turns/unfolded proteins)
	1440	Lipids	CH_2 scissoring/bending (lipids/proteins)
	1793	Lipids Carbohydrates	Ester C=O stretching (lipids, triglycerides, nucleic acid bases overlap)
Glucose-Glutamine	677	Proteins / Nucleic acids	C–S stretching (proteins), ring vibrations (Tyr, Trp, nucleic acid bases)
	695	Nucleic acids	Guanine/thymine ring vibrations
	965	Nucleic acids	DNA backbone phosphodiester symmetric stretching
	1035	Proteins	C–N stretching, skeletal modes (proteins)
	1062	Proteins Carbohydrates	C–C / C–N stretching, C–O stretching (carbohydrates, proteins)
	1406	Proteins / Lipids	CH_2/CH_3 bending (proteins, lipids)
	1520	Proteins	Amide II (N–H bending, C–N stretching)
	1440	Lipids	CH_2 scissoring/bending (lipids/proteins)
	1793	Lipids	Ester C=O stretching (lipids, triglycerides)

References

[1] Kerr LT, Hennelly BM. A multivariate statistical investigation of background subtraction algorithms for Raman spectra of cytology samples recorded on glass slides. Epub ahead of print 2016. DOI: 10.1016/j.chemolab.2016.08.012.

[2] Krafft C, Knetschke T, Funk RHW, et al. Studies on Stress-Induced Changes at the Subcellular Level by Raman Microspectroscopic Mapping. *Anal Chem* 2006; 78: 4424–4429.

[3] Notingher I. Raman Spectroscopy Cell-based Biosensors. *Sensors 2007, Vol 7, Pages 1343-1358* 2007; 7: 1343–1358.

[4] Raman Spectroscopy and Applications.